metals

MDPI

Article

Deposition of Arsenic from Nitric Acid Leaching Solutions of Gold–Arsenic Sulphide Concentrates

Kirill Karimov *, Denis Rogozhnikov, Evgeniy Kuzas, Oleg Dizer, Dmitry Golovkin and Maksim Tretiak

Department of Non-Ferrous Metals Metallurgy, Ural Federal University, 620002 Yekaterinburg, Russia; darogozhnikov@yandex.ru (D.R.); e.kuzas@ya.ru (E.K.); oleg.dizer@yandex.ru (O.D.); dmitry.golovkin@urfu.ru (D.G.); mtretyak144@gmail.com (M.T.)

* Correspondence: kirill_karimov07@mail.ru; Tel.: +7-912-695-3175

Abstract: At present, the processing of refractory gold–arsenic sulphide concentrates is becoming more relevant due to the depletion of rich crude ore reserves. In the process of the nitric acid leaching of arsenic sulphide minerals, solutions are formed containing 20–30 g/L of arsenic (III). Since market demand for arsenic compounds is limited, such solutions are traditionally converted into poorly soluble compounds. This paper describes the investigation of precipitating arsenic sulphide from nitric acid leaching solutions of refractory sulphide raw materials of nonferrous metals containing iron (III) ions using sodium hydrosulphide with a molar ratio of NaHS/As = 2.4–2.6, which is typical for pure model solutions without oxidants. The work studied the effect of temperature, the pH of the solution and the consumption of NaHS and seed crystal on this process. The highest degree of precipitation of arsenic (III) sulphide (95–99%) from nitric acid leaching solutions containing iron (III) ions without seed occurs with a pH from 1.8 to 2.0 and a NaHS/As molar ratio of 2.8. The introduction of seed crystal significantly improves the precipitation of arsenic (III) sulphide. An increase in seed crystal consumption from 0 to 34 g/L in solution promotes an increase in the degree of transition of arsenic to sediment from 36.2 to 98.1% at pH = 1. According to SEM/EDS and XRF sediment data, from the results of experiments on the effect of As_2S_3 seed crystal consumption, acidity and molar ratio of NaHS/As on the precipitation of arsenic (III) sulphide and the Fe_{total}/Fe^{2+} ratio in the final solution, it can be concluded that the addition of a seed accelerates the crystallisation of arsenic (III) sulphide by increasing the number of crystallisation centres; as a result, the deposition rate of As_2S_3 becomes higher. Since the oxidation rate of sulphide ions to elemental sulphur by iron (III) ions does not change significantly, the molar ratio of NaHS/As can be reduced to 2.25 to obtain a precipitate having a lower amount of elemental sulphur and a high arsenic content similar to that precipitated from pure model solutions.

Keywords: arsenic; trisulphide; precipitation; seed crystal consumption; nitric acid leaching; sodium hydrosulphide; elemental sulphur; mathematical model

Citation: Karimov, K.; Rogozhnikov, D.; Kuzas, E.; Dizer, O.; Golovkin, D.; Tretiak, M. Deposition of Arsenic from Nitric Acid Leaching Solutions of Gold–Arsenic Sulphide Concentrates. *Metals* **2021**, *11*, 889. https://doi.org/10.3390/met11060889

Academic Editors: Maria Luisa Blázquez Izquierdo, Jesús A. Muñoz Sánchez, Laura Castro and Jean François Blais

Received: 21 April 2021
Accepted: 26 May 2021
Published: 28 May 2021

1. Introduction

At present, the processing of refractory gold–arsenic sulphide concentrates is becoming more relevant due to the depletion of rich crude ore reserves. Within such processes, various pyro- and hydrometallurgical technologies are used to break down the sulphide matrix. However, when used with highly toxic arsenic raw materials, pyrometallurgical technologies (roasting, smelting, etc.) can be harmful to the environment because arsenic passes into the gas phase, concentrating in fine dust and dirty acid wastewater that requires additional processing technologies [1]. Conventional cyanide leaching of gold [2] may not always be viable without preliminary disintegration of the material. Among hydrometallurgical technologies for processing refractory sulphide raw materials, autoclave leaching [3–5] and bioleaching [6,7] are the most commonly used in world. These technologies provide a high efficiency of the target components extraction, but due to the complexity of the processes and capital intensity, their use is still limited.

Ultrafine grinding techniques are also widely used in order to intensify hydrometallurgical processes [8]. The Albion, Leachox and Activox processes are the most used [9–11]. The main difficulties and limitations of these technologies are the high energy costs associated with the need to obtain highly dispersed materials for hydrometallurgical processing. In this context, a promising area of research consists in nitric acid leaching [12–14].

Nitric acid is one of the most effective oxidizing and leaching agents [15]. Among the most famous technologies based on the use of HNO_3 are: the NSC process (nitrogen species-catalysed pressure leaching), Sunshine plant in the USA [16]; the Nitrox (in atmosphere air) and Arseno process (use of compressed oxygen) [17]; Redox (at above 180 °C to eliminate the formation of elemental S) [18]; the HMC process (a mixture of salts of nitric and hydrochloric acids) [19] and others.

The main advantages of using nitric acid in the leaching of such raw materials are the high efficiency of the process due to the exothermic reactions of sulphide oxidation with nitric acid and the possibility of completely evacuating the formed nitrous gases in the absorption system, followed by the regeneration of nitric acid [20–22].

In the process of the nitric acid leaching of refractory raw materials containing arsenopyrite, enargite, tennantite or other arsenic sulphide minerals, solutions are formed containing 20–30 g/L or more of arsenic (III). Since market demand for arsenic compounds is limited, such solutions are traditionally converted into poorly soluble compounds suitable for disposal in specially equipped landfills [23].

One of the simplest methods used to precipitate As (III) and As (V) solutions in the form of arsenites and calcium arsenates at pH 11–12 consists of their neutralisation with lime. It has been shown that the type and solubility of the resulting compound depend on the pH of the solution, as well as temperature, aging period and initial Ca:As molar ratio [24–26]. Although the lime precipitation process is a relatively economical method for immobilising arsenic, the resulting precipitation demonstrates poor long-term stability.

The precipitation of arsenic from iron solutions having an arsenate–ferrihydrite form is a promising approach due to the exceptional high stability of this compound according to the standard toxicity characteristic leaching procedure (TCLP) test (<0.5 mg/L). In this case, an increase in the Fe:As molar ratio results in greater stability. However, the presence of arsenic (III) requires the use of expensive oxidants (MnO_2, H_2O_2) to transform it into arsenic (V). Over prolonged storage, ferrihydrite begins to transform into goethite, which leads to the partial dissolution of arsenic [27].

Another common method for segregating arsenic consists in its precipitation into sulphide form. Thus, for example, weakly acidic effluents containing As (III) and solutions for processing converter dust from copper smelting production are neutralised with sodium hydrosulphide to fix As (III) in a sulphide form (As_2S_3), containing 30–60% arsenic [28–31]. As compared to the traditional neutralisation method, the production of arsenic (III) sulphide without the formation of free acid or the use of additional oxidants and lime as a neutraliser contributes to the production of a more concentrated arsenic sludge for a given volume. Arsenic trisulphide is stable under reducing conditions at pH < 4.

Despite the above-described advantages of the method of precipitation of arsenic in the form of As_2S_3, it has a number of limitations and is currently used mainly in the production of sulphuric acid for the purification of acidic wastes from effluent gases in copper smelting furnaces. The presence of oxidants and metal ions in a solution can result in increased consumption of expensive NaHS due to sulphide ion oxidation and the formation of insoluble metal sulphides.

The purpose of the present study is to demonstrate the possibility of precipitating arsenic sulphide from nitric acid leaching solutions of refractory sulphide raw materials of nonferrous metals containing iron (III) ions using sodium hydrosulphide with a molar consumption of NaHS/As = 2.4–2.6, which is typical for pure model solutions without oxidants [32,33]. In addition, the work studied the effect of temperature, the pH of the solution and the consumption of NaHS and seed crystal on this process. Combined with mathematical experiment planning methods, this allowed the process of precipitation of

arsenic sulphide from such multicomponent solutions to be described with high accuracy. The novelty of this study is the investigation of the arsenic sulphide precipitation from leaching solutions containing oxidants with minimization of sodium hydrosulphide oxidation.

2. Materials and Methods

2.1. Materials and Reagents

The study used solutions obtained after nitric acid leaching of gold–arsenic sulphide concentrates of the Uderey deposit (Krasnoyarsk Region), containing %: 21.6 Fe, 12.2 As, 20.0 S, 3.5 Al and 30 g/t Au [34,35]. The method and conditions of leaching were previously described in detail [34]. In order to remove free nitric acid as much as possible and increase the degree of its utilisation, a new batch of the concentrate with an excess (t = 80 °C) was added to the solution following leaching until the end of the evolution of nitrous gases, comprising products of the interaction of HNO_3 and sulphides, after which the pulp was allowed to stand for 30 min and then sent for filtration. The resulting solution had a pH = 1 and contained (g/L): 23.2 As (III), 29.0 As_{total}, 56.0 Fe_{total}, 4 Fe (II), 0.07 Cu, 0.1 Zn, 0.001 Pb, 8.5 NO_3^- and 161 SO_4^{2-}. Sulphate ions were obtained by nitric acid oxidation of sulphides. All subsequent experiments were carried out using this solution. For precipitation, a sodium sulphide solution containing 70 g/L NaHS was used [28,32,33,36].

The H_2SO_4 and NaOH used in this work were of analytical grade. The water was purified using a GFL distillation unit. In order to improve the reliability of the obtained results, each experiment was carried out twice.

2.2. Analysis

The chemical analysis of solid products of the studied processes was performed using an Axios MAX X-ray fluorescence spectrometer (XRF) (Malvern Panalytical Ltd., Almelo, The Netherlands). The chemical analysis of the obtained solutions was performed by mass spectrometry with inductively coupled plasma (ICP-MS) using an Elan 9000 Instrument (PerkinElmer Inc., Waltham, MA, USA). The phase analysis was performed on an XRD 7000 Maxima diffractometer (Shimadzu Corp., Tokyo, Japan).

Scanning electron microscopy (SEM) was performed using a JSM-6390LV microscope (JEOL Ltd., Tokyo, Japan) equipped with a module for energy-dispersive X-ray spectroscopy analysis (EDS).

Samples from each experiment were taken and analysed using inductively coupled plasma mass spectrometry (ICP-MS—NexION 300S quadrupole mass spectrometer, PerkinElmer Inc., Waltham, MA, USA). The Fe (II) concentration in the solution was determined by potassium dichromate ($K_2Cr_2O_7$) titration. For the aqueous samples containing both As (III) and Fe (II), they were separated using an ion exchange column and then determined by titration [37]. To determine the Fe (II) concentration, transfer the sample solution into an Erlenmeyer flask. Using a graduated cylinder, add 25 mL of 1 M H_2SO_4 to flask. Then, add 10 cm^3 of the phosphoric acid solution and 8 drops of sodium diphenylamine sulfonate indicator to the flask. The intense purple colour produced by the first drop of excess $K_2Cr_2O_7$ signals the end point for the titration.

In order to obtain regression equations and Pareto diagrams, experimental data were processed using the Statgraphics Centurion Software Version 18 (Statgraphics Technologies, Inc., The Plains, VA, USA).

The Pourbaix diagram was constructed using the HSC Chemistry Software Version 6.0 (Outokumpu Research Oy, Finland).

2.3. Experimental Procedure

A solution comprising a volume of 200 mL was poured into a thermostated reactor. After reaching the required temperature, stirring was switched on, and the supply of sodium hydrosulphide was started according to the assumption that the arsenic sulphide precipitation process lasts for about 1 hour. The pH of the system was changed by adding

a diluted 1:1 solution of H_2SO_4 (7.1 M) and NaOH (8.1 M). Following the completion of the precipitation process, the pulp was allowed to stand for 10–20 min to undergo exchange reactions between iron and arsenic. Next, the pulp was filtered to form cakes, which were dried at a temperature of 60 °C to a constant sediment mass.

3. Results and Discussion

3.1. Thermodynamics of Arsenic Sulphide Precipitation

The reaction mechanism according to which arsenic precipitates from acidic solutions in sulphide form has been described in previous studies [32,38,39]:

$$2NaHS(l) + H_2SO_4(l) = 2H_2S(g) + Na_2SO_4(l)\ (\Delta G^0{}_{298} = -61.85\ kJ/mol), \quad (1)$$

$$3H_2S(g) + 2H_3AsO_3(l) = As_2S_3(s)\downarrow + 6H_2O(l)\ (\Delta G^0{}_{298} = -137.59\ kJ/mol), \quad (2)$$

$$H_2S(g) + H_3AsO_4(l) = S^0(s)\downarrow + H_3AsO_3(l) + H_2O(l)\ (\Delta G^0{}_{298} = -82.38\ kJ/mol), \quad (3)$$

$$5H_2S(g) + 2H_3AsO_4(l) = As_2S_5(s)\downarrow + 8H_2O(l)\ (\Delta G^0{}_{298} = -77.25\ kJ/mol). \quad (4)$$

According to these reactions, when sodium hydrosulphide enters an acidic environment, it decomposes to hydrogen sulphide, which in turn interacts with arsenic (III) ions to form insoluble As_2S_3.

Data obtained from previous studies have shown [32,39,40] that the precipitation of arsenic (V) from solutions takes place in two stages. At the first stage, arsenic (V) ions oxidise sulphide ions to elemental sulphur, reducing to As (III) (Reaction 4). At the second stage, As_2S_3 is precipitated according to Reaction 1. Since the rate of reduction of As (V) to As (III) is much lower than the rate of formation of As_2S_3, the process is limited by the first stage [24,32]. Despite the negative values of the Gibbs energy change, As_2S_5 does not form significantly in acidic media due to its solubility being higher than that of As_2S_3 (the solubility is 4.4×10^{-6} and 8.13×10^{-7} M, respectively) [41]. This is also confirmed by the data presented in the Pourbaix diagram (Figure 1). Concentrations of As, S and Fe are 1 mol/dm^3.

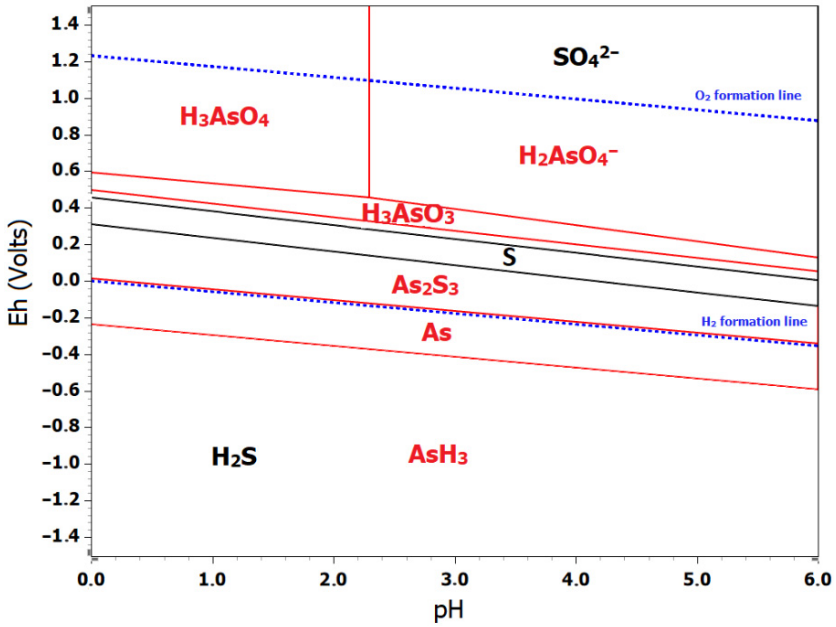

Figure 1. Pourbaix diagram of As-S-H_2O system at 25 °C.

Within the considered pH range, the arsenic sulphide field is within the redox potential from −0.2 to 0.5 V. According to the data of previous studies, with an increase in the molar ratio S:As $\geq$ 1.5, the range of existence of As_2S_3 expands within the oxidation potential from 0 to 1.1 V at pH from 0 to 6 [32].

In solutions containing iron (III) ions, sulphide ion can be oxidised to elemental sulphur with the formation of iron (II) ions, according to the following reaction:

$$H_2S(g) + Fe_2(SO_4)_3(l) = 2FeSO_4(l) + H_2SO_4(l) + S^0(s)\downarrow (\Delta G^0{}_{298} = -41.9 \text{ kJ/mol}). \quad (5)$$

$$H_2S(g) + 2Fe(NO_3)_3(l) = 2Fe(NO_3)_2(l) + 2HNO_3(l) + S^0(s)\downarrow (\Delta G^0{}_{298} = -54.98 \text{ kJ/mol}). \quad (6)$$

$$2FeSO_4(l) + 2HNO_3(l) + H_2SO_4(l) = Fe_2(SO_4)_3(l) + 2NO_2(g) + 2H_2O(l) (\Delta G^0{}_{298} = -113.7 \text{ kJ/mol}). \quad (7)$$

$$H_2S(g) + 2HNO_3(l) = 2NO_2(g) + S^0(s)\downarrow + 2H_2O(l) (\Delta G^0{}_{298} = -177.1 \text{ kJ/mol}). \quad (8)$$

3.2. Influence of the Main Parameters Governing the Precipitation of Arsenic (III) Sulphide from Nitric Acid Leaching Solutions on the Degree of Reduction of Fe^{3+} Ions to Fe^{2+}

According to the results of previous studies, the complete removal of arsenic in the case of its precipitation from pure model solutions containing As (III) is achieved at a NaHS/As molar ratio $\geq$ 2.5. Although the stoichiometrically required ratio of NaHS/As is 1.5, in this case, arsenic is precipitated by a ratio of only 70% [32,33]. The As (V)/As (III) ratio in solution—i.e., the above-described process of As (V) reduction to As (III) [32,39,40]—has a significant influence on the kinetics of the process.

3.2.1. Effect of pH and NaHS/As Molar Ratio

In order to study the effect of pH and molar ratio of NaHS/As on the precipitation of arsenic from nitric acid leaching solutions containing iron (III) ions in the form As_2S_3, we used a mathematical experimental planning approach involving second-order orthogonal central compositional design [36,42–44]. The variable parameters were the pH (X_1) and NaHS/As molar flow rate (X_2). The temperature of 25 °C and duration of 1 h were constant.

Two parameters at five levels, considered as independent variables, had central values (zero levels) as follows: $X_1 = 1.25$; $X_2 = 1.91$. Table 1 shows the results of design experiments performed to evaluate the dependent variable (arsenic deposition rate). The processing of experimental data to obtain a mathematical model and Pareto diagram was carried out using the Statgraphics program. The optimal pH and NaHS/As molar ratio values were selected using program data and graphical optimisation tools [42–44].

Table 1. Central composite design arrangement and results.

Experimental Runs	pH	Molar Ratio (NaHS/As)	Precipitation Degree of As, %	Concentration in Solution, g/L	
				Fe^{2+}	Fe_{total}
1	0.34	1.91	16.4	28.3	46.4
2	0.50	1.22	14.9	13.9	45.3
3	0.50	2.60	24.1	27.0	41.8
4	1.25	1.08	13.3	12.6	53.8
5	1.25	1.91	19.1	22.6	56.3
6	1.25	1.91	22.4	23.3	57.4
7	1.25	1.91	21.7	25.6	57.7
8	1.25	1.91	22.0	24.0	57.0
9	1.25	2.74	37.6	30.4	43.6
10	2.00	1.22	14.2	22.6	46.0
11	2.00	2.60	99.2	32.0	43.9
12	2.16	1.91	59.3	31.8	49.6

Based on the model sum of squares, the highest order polynomial was selected as the experimental model. This model is significant and not aliased. To assess the variance and accuracy of the model, a correlation coefficient of 0.96 was used; this indicated that independent variables having a probability of 96% describe the change in the degree of precipitation of arsenic from the solution.

Table 2 determines the statistical significance of each coefficient of the equation by comparing the mean square against the experimental error estimate. According to the obtained data, four coefficients have a *p*-value less than 0.05, which confirms their significance at a confidence level of 95.0%. The coefficient X_2^2 is not statistically significant due to the *p*-value being greater than 0.05. The significance of each coefficient is presented on the Pareto chart (Figure 2).

Table 2. Analysis of variance (ANOVA) of the response surface quadratic model.

Source	Sum of Squares	Degree of Freedom	Mean Square	F-Ratio	*p*-Value
X_1	2302.76	1.00	2302.76	42.39	0.0006
X_2	2205.15	1.00	2205.15	40.59	0.0007
X_1^2	654.26	1.00	654.26	12.04	0.0133
X_1X_2	1436.41	1.00	1436.41	26.44	0.0021
X_2^2	64.68	1.00	64.68	1.19	0.3171
Total error	325.94	6.00	54.32	-	-
Total (corr.)	6989.19	11.00	-	-	-

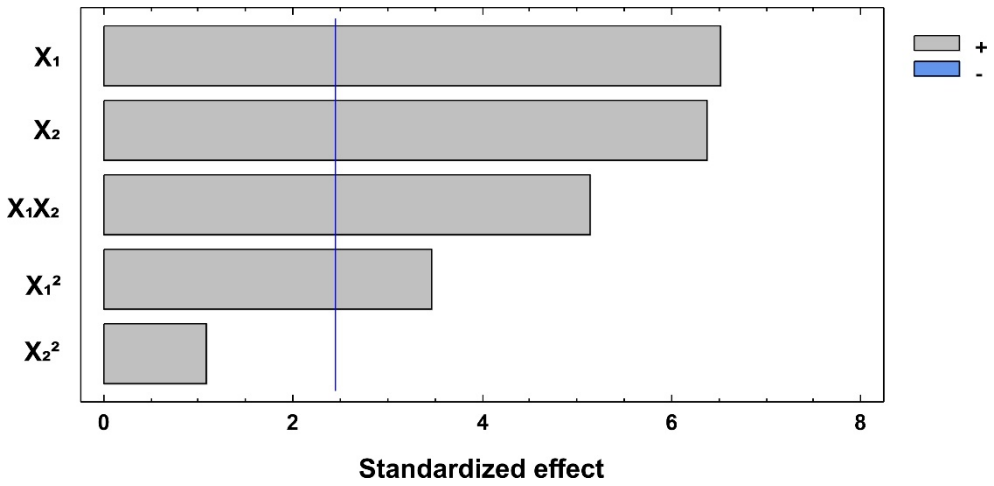

Figure 2. Pareto chart for arsenic sulphide precipitation.

The pH and NaHS/As molar flow rate have almost equal influence on the precipitation of arsenic (III) sulphide; the coefficient X_2^2 is not statistically significant (Figure 2).

The obtained mathematical model for the precipitation of arsenic sulphide from nitric acid leaching solutions containing iron (III) ions can be described by the equation presented below on a dimensional scale:

$$\text{As (\%)} = 92.71 - 100.54X_1 - 51.08X_2 + 21.96X_1^2 + 36.62X_1X_2. \quad (9)$$

Figure 3 shows the relationship between the actual arsenic deposition values and those predicted by the model: the reliability of the chosen model (Equation (9)) is confirmed due to the close coincidence of the predicted and actual data.

Figure 4 shows the predicted model response surface for the degree of precipitation of arsenic (III) sulphide from nitric acid leach solutions containing iron (III) ions depending on pH and the NaHS/As molar flow rate at 25 °C.

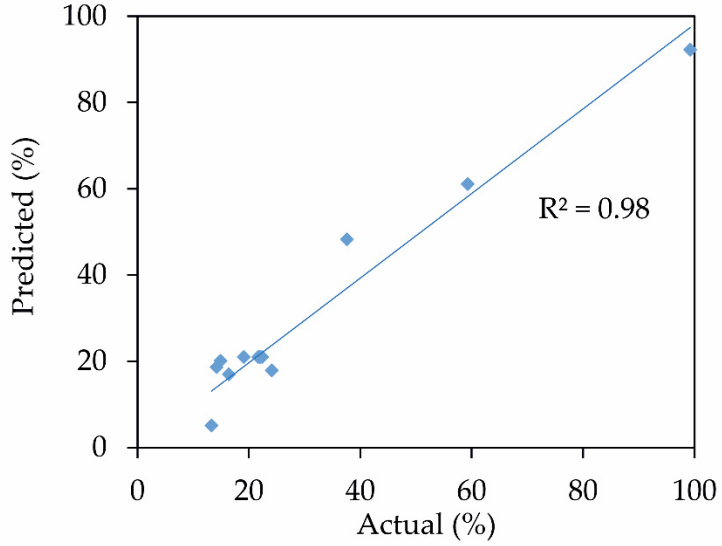

Figure 3. Real and predicted values of the removal efficiency of arsenic (III).

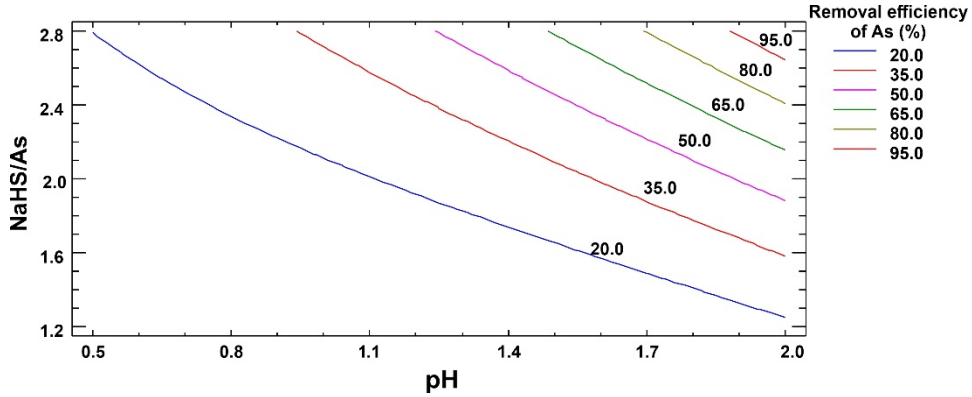

Figure 4. Dependence of the removal efficiency of arsenic (III) sulphide on pH and molar ratio of NaHS/As (contour response surface).

From the data presented in Figure 4, it follows that the precipitation of arsenic (III) sulphide from nitric acid leaching solutions is significantly influenced by both considered parameters. The deposition of arsenic above 50% is observed only at pH > 1.2. A noticeable (20%) precipitation of arsenic (III) sulphide with a stoichiometric consumption of NaHS/As = 1.5 begins only at pH 1.7. An increase in pH to 2.0 promotes an increase in the transition of arsenic to a precipitate up to 30%. These data differ significantly from the results of precipitation from model solutions, from which, according to previous studies, up to 70% As was extracted from the solution under identical conditions [32,33]. This effect can be associated with the oxidation of the sulphide ion by iron (III) ions to elemental sulphur according to Reactions 5 and 6. For the removal of 96–99% of arsenic (III) from pure model solutions, a consumption of NaHS/As = 2.4–2.5 is required. The highest degree of precipitation of arsenic (III) sulphide (95–99%) from nitric acid leaching solutions containing iron (III) ions can be seen in the range of pH from 1.8 to 2.0 with a NaHS/As molar ratio of 2.8. The difference from model solutions can be attributed to the influence of iron (III) ions present in the solution.

The analysis of the effect of pH and molar ratio of NaHS/As on the degree of reduction of iron (III) ions to iron (II) at 25 °C is shown in Figure 5. In order to compare the results, we used the ratio of the total amount of iron in solution to iron (II) (Fe_{total}/Fe^{2+}).

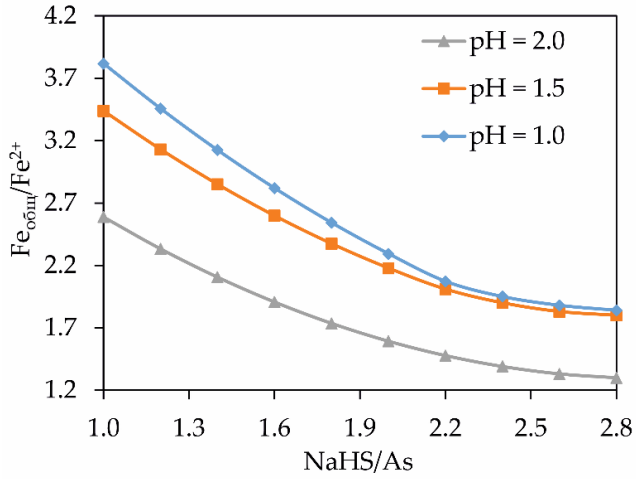

Figure 5. Dependence of the Fe_{total}/Fe^{2+} ratio on the molar ratio of NaHS/As at different pH values and 25 °C.

The increase in the molar ratio of NaHS/As, which is due to the oxidation of the sulphide ion by iron (III) ions to elemental sulphur according to Reactions 5 and 6 (Figure 5), contributes to a decrease in the Fe_{total}/Fe^{2+} ratio. The pH of the solution has a significant influence on the reduction of iron (III) ions. An increase in pH leads to a decrease in the Fe_{total}/Fe^{2+} ratio in solution, promoting the oxidation of the sulphide ion and an increase in the NaHS/As molar ratio, which in turn negatively affects the precipitation of arsenic (III) sulphide.

The values of the Fe_{total}/Fe^{2+} ratio at pH = 1.0–1.5 become almost identical, with an increase in the NaHS/As molar flow rate from 1.0 to 2.2. An increase in pH from 1.5 to 2.0 leads to a sharp decrease in the Fe_{total}/Fe^{2+} ratio, which, at the NaHS/As molar ratio of 2.8 required for the precipitation of 95–99% As, is 1.25. This indicates an almost complete reduction of iron (III) ions to iron (II).

3.2.2. Influence of Temperature

The effect of temperature on the degree of precipitation of arsenic (III) sulphide from nitric acid leaching solutions containing iron (III) ions and the value of the ratio Fe_{total}/Fe^{2+} in solution at a molar flow rate of NaHS/As = 2.8 are shown in Figure 6.

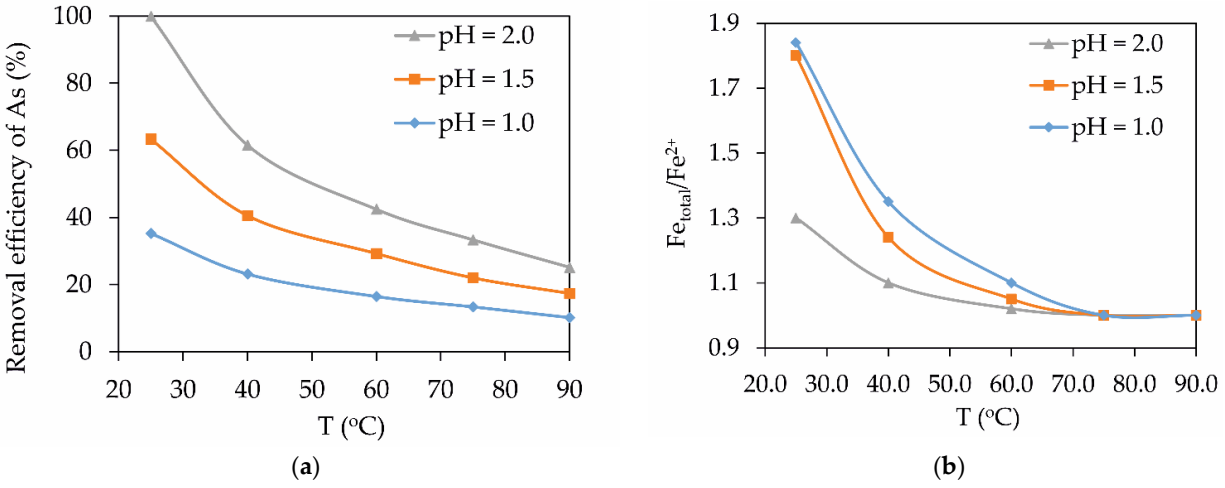

Figure 6. Dependence of the removal efficiency of arsenic (III) sulphide (**a**) and the ratio Fe_{total}/Fe^{2+} (**b**) in solution on temperature at a molar ratio of NaHS/As = 2.8.

From the data in Figure 6a, it can be seen that an increase in temperature leads to a significant decrease in the deposition of arsenic (III) sulphide, which is different from that obtained when precipitating arsenic from pure model solutions [33]. As the temperature rises from 25 to 60 °C, the degree of arsenic transfer to the precipitate is almost halved for the entire studied pH range from 1.0–2.0. This is due to an increase in the oxidation state of the sulphide ion by iron (III) ions to elemental sulphur, which is also confirmed by a decrease in the ratio Fe_{total}/Fe^{2+} in solution to 1.05–1.01 (Figure 6b), indicating the complete reduction of iron ions (III) to iron (II).

3.2.3. Influence of As_2S_3 Seed Crystal Consumption

For seed crystal purposes, we used arsenic sulphide precipitated from solutions of nitric acid leaching at a temperature of 25 °C, a pH of 2 and a NaHS/As molar flow rate of 2.8 having the composition (%): As–34.8; S–53.1; Fe–1.1; Cu–0.2; Zn–0.3.

The effect of temperature on the degree of precipitation of arsenic (III) sulphide from nitric acid leaching solutions containing iron (III) ions and the value of the ratio Fe_{total}/Fe^{2+} in solution at a molar flow rate of NaHS/As = 2.8 is shown in Figure 7.

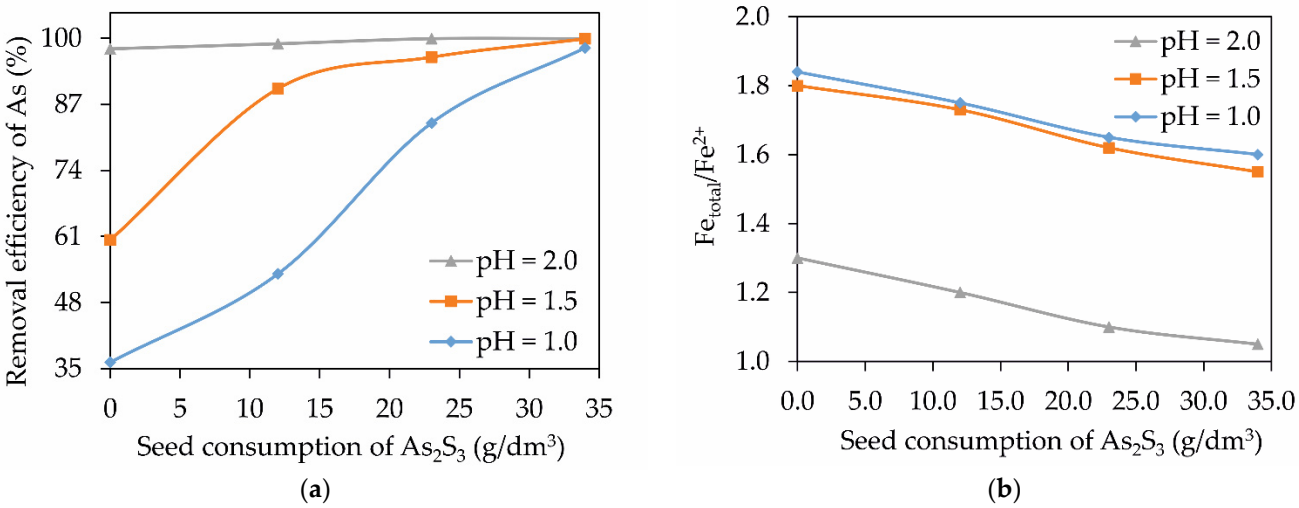

Figure 7. Dependence of the removal efficiency of arsenic (III) sulphide (**a**) and the ratio Fe_{total}/Fe^{2+} (**b**) in solution on seed crystal consumption at a molar NaHS/As consumption of 2.8 and a temperature of 25 °C.

From Figure 7a, it can be seen that the introduction of seed crystal significantly improves the precipitation of arsenic (III) sulphide. An increase in the seed consumption from 0 to 34 g/L in the solution increases the degree of arsenic transfer to sediment from 36.2 to 98.1% at pH = 1. The solubility of arsenic (III) sulphide decreases with decreasing acidity and is minimal at pH = 4 [38]. Thus, an increase in the pH of the solution from 1 to 2 leads to a decrease in the solubility of arsenic (III) sulphide to produce a supersaturated solution. This leads to the formation of solid phase nuclei capable of reaching a critical size and serving as crystallization centres, whose further growth, initially accompanied by a decrease in the Gibbs energy, then proceeds spontaneously. The positive effect of increasing the pH of the solution can also be associated with an increase in the formation of solid particles of elemental sulphur, as indicated by an increase in the concentration of iron (II) ions in the solution (Figure 7b) or iron hydroxide, which can serve as additional crystallisation centres for arsenic (III) sulphide. The introduction of the As_2S_3 seed crystal neutralises the effect of pH on the precipitation of arsenic (III) sulphide by increasing the number of its crystallisation centres.

Figure 7b shows that an increase in the consumption of As_2S_3 seed crystal promotes a decrease in the Fe_{total}/Fe^{2+} ratio in a solution with the same molar ratio of NaHS/As = 2.8. For pH = 1.0–1.5, the Fe_{total}/Fe^{2+} ratio decreases from 1.84 to 1.55, while at pH = 2.0 it decreases from 1.30 to 1.05. According to the literature data, the oxidation of arsenic (III)

sulphide by iron (III) ions in Reaction 10 at a temperature of 25 °C also occurs at a low rate [45]. This effect can also be associated with sorption and the mechanical capture by the developed surface of the precipitated arsenic (III) sulphide of compounds $H_3As_3S_6$ and $H_2As_4S_7$. When a crystal seed is added to the solution, these compounds dissociate with the formation of H_2S, according to Reactions 11 and 12, which in turn can interact with iron (III) and arsenic (V) ions according to Reactions 3, 5 and 6 [24,39,46].

$$As_2S_3(s)\downarrow + 1.5Fe_2(SO_4)_3(l) + 4H_2O(l) = 2H_3AsO_3(l) + 3.5S(s)\downarrow + 3FeSO_4(l) + H_2SO_4(l), \quad (10)$$

$$H_2As_3S_6(l) + H^+ + 9H_2O(l) = 3H_3AsO_3(l) + 6H_2S(g), \quad (11)$$

$$HAs_4S_7(l) + H^+ + 12H_2O(l) = 4H_3AsO_3(l) + 7H_2S(g). \quad (12)$$

The introduction of As_2S_3 mitigates the effect of pH on the precipitation of arsenic (III) sulphide, while the oxidation state of sulphide ions to elemental sulphur decreases with decreasing pH due to an increase in the ratio Fe_{total}/Fe^{2+} in the final solution. In order to reduce the NaHS/As molar ratio, the effect of As_2S_3 34 g/L seed crystal consumption on the degree of precipitation of arsenic (III) sulphide at a temperature of 25 °C, pH = 1.5 was investigated. The results are shown in Figure 8.

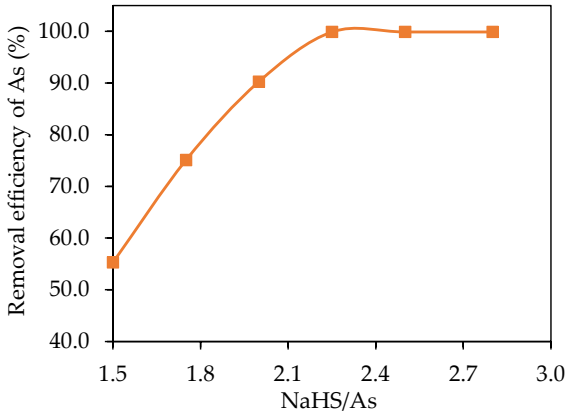

Figure 8. Dependence of the removal efficiency of arsenic (III) sulphide on the NaHS/As molar ratio at 25 °C, pH = 1.5 and As_2S_3 seed consumption = 34 g/L.

The maximum precipitation of arsenic (III) sulphide of 99.9% is achieved at a molar flow rate of NaHS/As = 2.25 and does not change significantly with its further increase. Thus, the introduction of the As_2S_3 seed crystal in an amount of 34 g/L at pH = 1.5 allows the molar ratio of NaHS/As to be reduced from 2.80 to 2.25 by decreasing the oxidation state of sulphide ions to elemental sulphur by iron ions (III).

3.3. Residue Characteristics

Changes in the morphology and composition of the sample depending on the experimental conditions were assessed using XRD and SEM–EDS methods to study the cakes obtained after precipitation of arsenic (III) sulphide from nitric acid leaching solutions containing iron (III) ions. Micrographs of the sediments obtained with and without the introduction of As_2S_3 seed crystal at a temperature of 25 °C and a pH of 1.5 are shown in Figure 9. The chemical composition of the sediments is presented in Table 3.

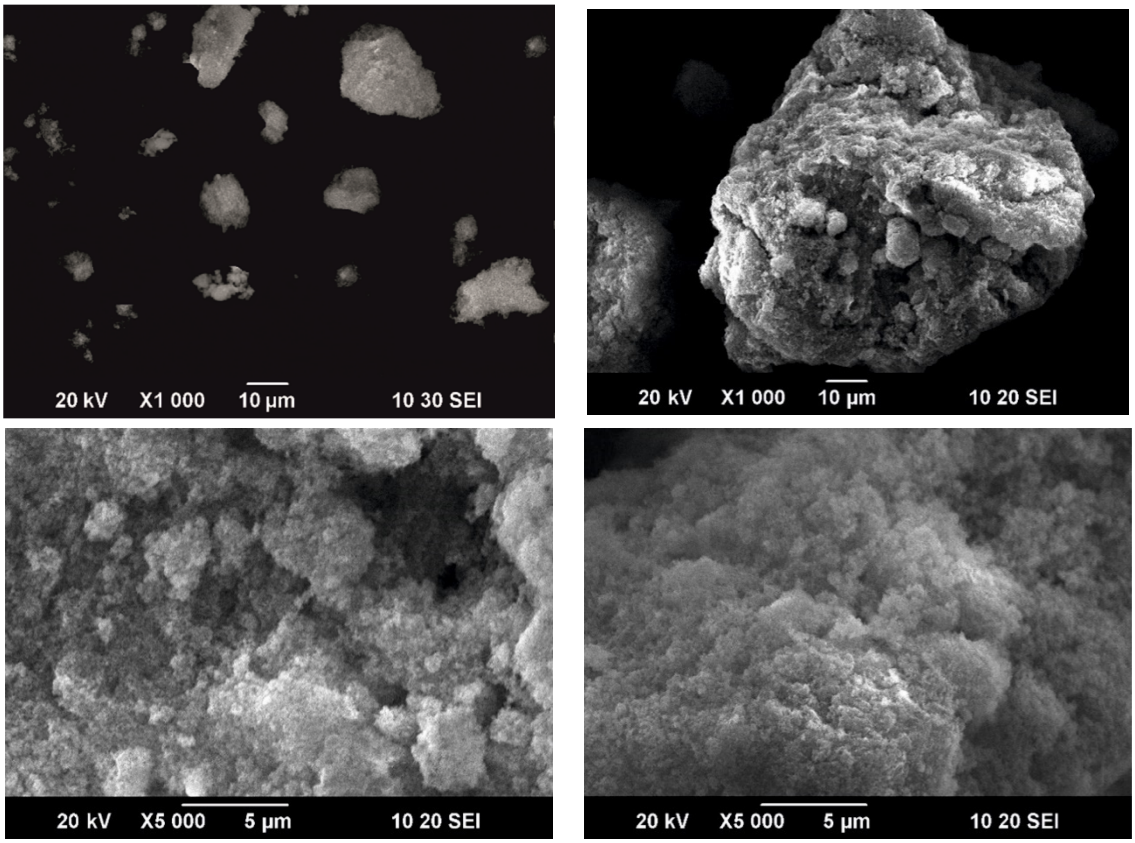

Figure 9. Micrographs of precipitates obtained without seed crystal introduction at NaHS/As = 2.80 (**a**) and with the introduction of As_2S_3 34 g/L seed crystal at NaHS/As = 2.25 (**b**).

Table 3. Chemical composition of arsenic trisulphide, wt%.

Material	As	S	Fe	Zn	Cu
Without seed	34.8	53.1	1.1	0.2	0.3
With seed	42.2	42.9	0.9	0.2	0.2

According to the data in Table 3, the precipitate of arsenic (III) sulphide obtained without introducing seed crystal is characterised by an increased sulphur content and a reduced arsenic content relative to the precipitate obtained at a consumption of As_2S_3 seed crystal of 34 g/L. As a result, the precipitation of arsenic (III) sulphide from nitric acid leaching solutions containing iron (III) ions at a temperature of 25 °C, a pH of 1.5 and an As_2S_3 seed consumption of 34 g/L results in a sediment that is similar in chemical and phase composition to cakes obtained from pure model solutions with a reduced molar ratio of NaHS/As = 2.25 (for model solutions NaHS/As = 2.5), containing 25–36% sulphur [32,33].

From the micrographs (Figure 9), it can be seen that the precipitation, which does not significantly vary, is represented by variously shaped agglomerates, having a porous, rough and very developed surface (Figure 9a,b). As confirmed by the X-ray phase analysis data shown in Figure 10, this is due to the low level of crystallinity of the sediments.

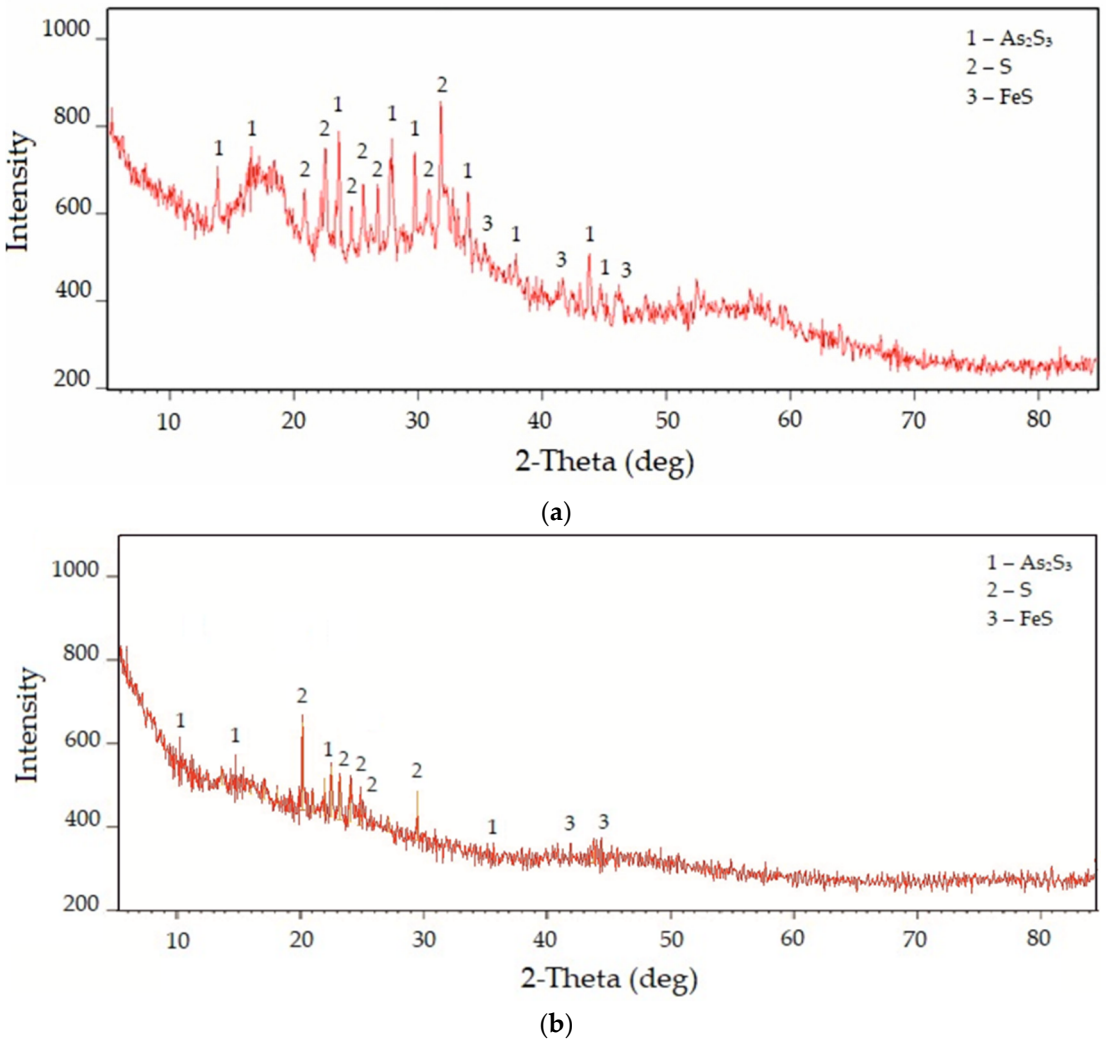

Figure 10. Diffraction pattern of the obtained precipitates of arsenic (III) sulphide with the introduction of As_2S_3 seed crystal in the amount of 34 g/L (**a**) and without seed crystal introduction (**b**).

The large amount of noise in the X-ray diffraction patterns is due to the low level of crystallinity of the resulting As_2S_3 precipitate. The sediment contains a significant amount of elemental sulphur along with traces of FeS (Figure 10). The presence of such a quantity of elemental sulphur can be explained in terms of the oxidation of sulphide ions by iron (III) and arsenic (V) ions according to Reactions 3, 5 and 6. The presence of only As_2S_3 in the sediment confirms the data of thermodynamic studies into the mechanism of the precipitation of arsenic (V) from solutions in two stages according to Reactions 2 and 3.

The micrographs and points of composition determined using energy-dispersive X-ray spectroscopy (Figure 11) are shown both for sediments obtained without the introduction of As_2S_3 seed crystal and for those obtained with its introduction at a temperature of 25 °C and a pH of 1.5 (Table 4).

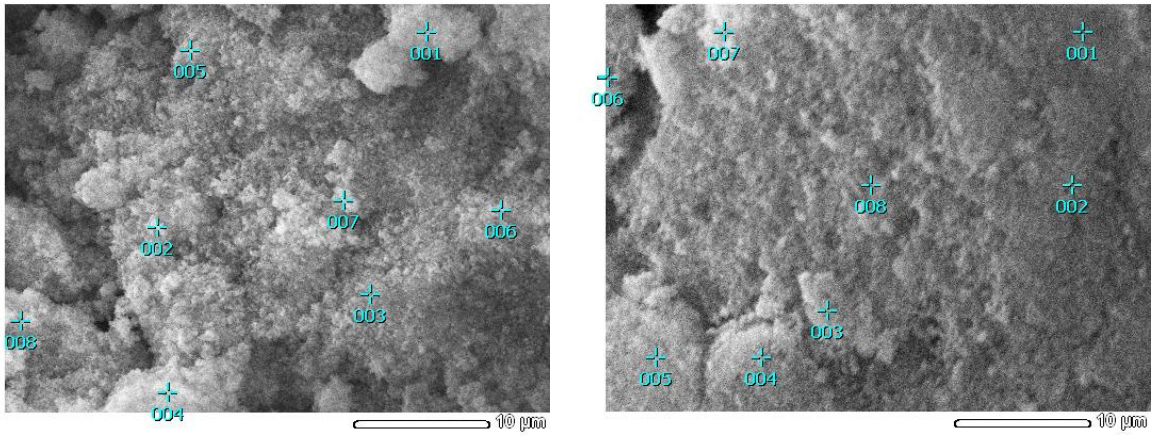

(**a**) (**b**)

Figure 11. Micrographs with composition determination points for sediments of arsenic (III) sulphide with the introduction of As_2S_3 seed crystal in the amount of 34 g/L (**a**) and without seeding (**b**).

Table 4. The results of energy dispersive spectroscopy, wt%.

Element	S	As	Total
Figure 11a. Point 001	87.8	12.2	100.0
Figure 11a. Point 002	62.6	37.4	100.0
Figure 11a. Point 003	57.3	42.7	100.0
Figure 11a. Point 004	82.7	17.3	100.0
Figure 11a. Point 005	69.8	30.2	100.0
Figure 11a. Point 006	58.9	41.1	100.0
Figure 11a. Point 007	64.8	35.2	100.0
Figure 11a. Point 008	74.6	25.4	100.0
Figure 11b. Point 001	54.8	45.2	100.0
Figure 11b. Point 002	56.5	43.5	100.0
Figure 11b. Point 003	51.8	48.2	100.0
Figure 11b. Point 004	54.1	45.9	100.0
Figure 11b. Point 005	55.4	44.6	100.0
Figure 11b. Point 006	52.7	47.3	100.0
Figure 11b. Point 007	53.4	46.6	100.0
Figure 11b. Point 008	55.8	44.2	100.0

Arsenic (III) sulphide particles do not have any films on their surface. The nonuniform distribution of sulphur and arsenic shown in Figure 11b is due to the oxidation of sulphide ions to elemental sulphur by iron (III) and arsenic (V) ions according to Reactions 3, 5 and 6 in the case of running the process without seeding. With an As_2S_3 seed consumption of 34 g/L, a more homogeneous sediment containing a lower amount of sulphur (Figure 11a) is formed as confirmed by the EDS results.

According to Figure 12, the sulphur content on the surface of the particles increases during the deposition without seeding, while arsenic content decreases.

The micrograph, X-ray phase analysis and EDS mapping data confirm a decrease in the content of elemental sulphur on the surface of particles and an increase in the content of arsenic in the sediment when using As_2S_3 crystal seeding.

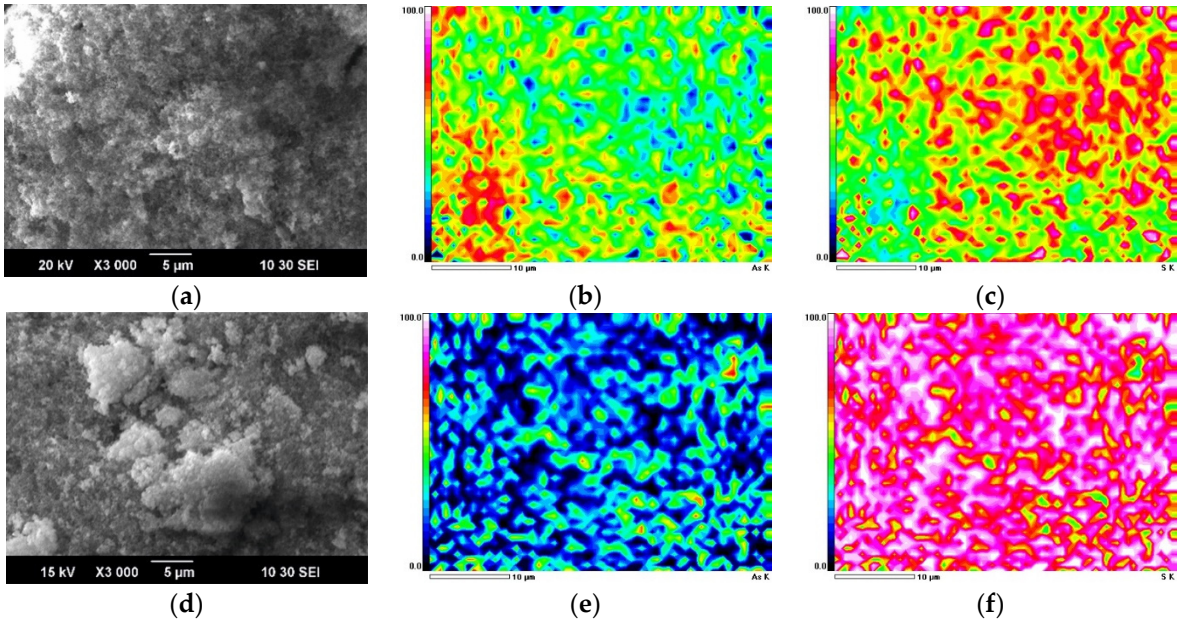

Figure 12. Micrographs of arsenic (III) sulphide precipitates with the introduction of As_2S_3 at 34 g/L (**a**) and without its introduction (**d**); EDS mapping for arsenic (**b**,**e**) and sulphur (**c**,**f**).

According to the precipitation analysis showing the influence of the As_2S_3 seed crystal consumption, acidity and molar ratio of NaHS/As on the degree of the precipitation of arsenic (III) sulphide and the ratio Fe_{total}/Fe^{2+} in the final solution, it can be concluded that the addition of seed crystal accelerates the process of arsenic (III) sulphide crystallization by increasing the number of crystallization centres. As a result, the deposition rate of As_2S_3 increases, while the oxidation rate of sulphide ions to elemental sulphur by iron (III) ions does not change significantly. This, in turn, allows the molar ratio of NaHS/As to be reduced to 2.25 to obtain a precipitate with less elemental sulphur and a high arsenic content similar to that obtained when precipitating arsenic from pure model solutions.

The flowchart of the leaching and further arsenic (III) sulphide precipitation processes is shown in Figure 13.

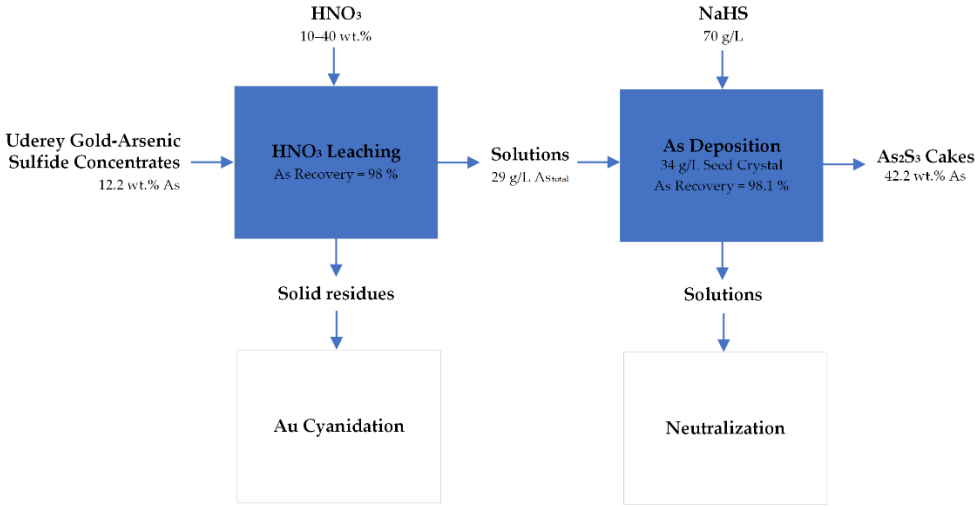

Figure 13. The flowchart of the leaching and further arsenic (III) sulphide precipitation processes.

The applications of these research results in industry would allow for a reduction in the consumption of expensive NaHS.

The hydrothermal mineralization stabilization can be adopted to improve the stability of amorphous As_2S_3. The results showed that the As leaching concentration of mineralized As_2S_3 was only 4.82 mg/dm^3. Furthermore, the amorphous As_2S_3 could be transformed into crystallized As_2S_3 (orpiment) in the presence of the mineralizer Na_2SO_4. Simultaneously, the As leaching concentration of crystallized As_2S_3 was further reduced to 3.86 mg/dm^3 [33].

4. Conclusions

The study investigated the process of the precipitation of arsenic (III) sulphide from multicomponent solutions of nitric acid leaching of refractory sulphide raw materials of nonferrous metals containing iron (III) ions. As a result, the following conclusions were drawn:

- The highest degree of precipitation of arsenic (III) sulphide (95–99%) from nitric acid leaching solutions containing iron (III) ions occurs with a pH from 1.8 to 2.0 and a NaHS/As molar ratio of 2.8. An increase in the molar ratio of NaHS/As and pH promotes a decrease in the Fe_{total}/Fe^{2+} ratio due to the oxidation of the sulphide ion by iron (III) ions to elemental sulphur.
- An increase in temperature leads to a significant decrease in the precipitation of arsenic (III) sulphide. As the temperature rises from 25 to 60 °C, the degree of arsenic transfer to the precipitate is almost halved for the entire studied pH range from 1.0 to 2.0. This is due to an increase in the oxidation state of the sulphide ion by iron (III) ions to elemental sulphur, which is also confirmed by a decrease in the Fe_{total}/Fe^{2+} ratio in solution to 1.05–1.01.
- The introduction of seed crystal significantly improves the precipitation of arsenic (III) sulphide. An increase in seed crystal consumption from 0 to 34 g/L in solution promotes an increase in the degree of transition of arsenic to sediment from 36.2 to 98.1% at pH = 1.
- According to SEM/EDS and XRF sediment data, from the results of the experiments on the effect of As_2S_3 seed crystal consumption, acidity and molar ratio of NaHS/As on the precipitation of arsenic (III) sulphide and the Fe_{total}/Fe^{2+} ratio in the final solution, it can be concluded that the addition of a seed accelerates the crystallisation of arsenic (III) sulphide by increasing the number of crystallisation centres; as a result, the deposition rate of As_2S_3 becomes higher. Since the oxidation rate of sulphide ions to elemental sulphur by iron (III) ions does not change significantly, the molar ratio of NaHS/As can be reduced to 2.25 to obtain a precipitate having a lower amount of elemental sulphur and a high arsenic content similar to that precipitated from pure model solutions.
- As compared to the traditional neutralisation method, the production of arsenic (III) sulphide without the formation of free acid or the use of additional oxidants and lime as a neutraliser contributes to the production of a more concentrated arsenic sludge for a given volume containing 42% arsenic. Arsenic trisulphide is stable under reducing conditions at pH < 4.

Author Contributions: Conceptualization, D.R.; data curation, E.K.; investigation, O.D., D.G. and M.T.; writing—review and editing, K.K. All authors have read and agreed to the published version of the manuscript.

Funding: This work was financially supported by the Russian Science Foundation Project No. 20-79-00321. The SEM–EDS analyses were funded by State Assignment, Grant No. 0836-2020-0020.

Institutional Review Board Statement: Not applicable.

Informed Consent Statement: Not applicable.

Data Availability Statement: Data is contained within the article.

Conflicts of Interest: The authors declare no conflict of interest.

References

1. Brittan, M. Oxygen roasting of refractory gold ores. *Miner. Eng.* **1995**, *47*, 145–148. [CrossRef]
2. Vikentyev, I.V. Invisible and microscopic gold in pyrite: Methods and new data for massive sulfide ores of the Urals. *Geol. Ore Depos.* **2015**, *57*, 237–265. [CrossRef]
3. Rusanen, L.; Aromaa, J.; Forsen, O. Pressure oxidation of pyrite-arsenopyrite refractory gold concentrate. *Physicochem. Probl. Miner. Process.* **2013**, *49*, 101–109. [CrossRef]
4. Conner, K.D. Pressure Oxidation of Enargite Concentrates Containing Gold and Silver. Ph.D. Thesis, Colorado School of Mines, Golden, CO, USA, 2014; pp. 1–366.
5. Zaytsev, P.; Fomenko, I.; Chugaev, V.L.; Shneerson, M.Y. Pressure oxidation of double refractory raw materials in the presence of limestone. *Tsvetn. Met.* **2015**, *105*, 41–49. [CrossRef]
6. Miller, P.; Brown, A. Bacterial oxidation of refractory gold concentrates. *Dev. Miner. Process.* **2005**, *15*, 371–402. [CrossRef]
7. Harvey, T.J.; Bath, M. The GeoBiotics GEOCOAT® Technology–Progress and Challenges. In *Biomining*; Rawlings, D.E., Johnson, D.B., Eds.; Springer: Berlin/Heidelberg, Germany, 2007; pp. 97–112. [CrossRef]
8. Johnson, G.; Corrans, I.; Angove, J. The Activox™ Process for Refractory Gold Ores. In Proceedings of the Randol Gold Forum, Beaver Creek, CO, USA, 7–9 September 1993; pp. 183–189.
9. Hourn, M. Refractory leaching solutions. *Aust. Min.* **2009**, *101*, 20.
10. Leachox Process. Available online: https://zolotodb.ru/article/12208 (accessed on 10 May 2021).
11. McDonald, R.G.; Muir, D.M. Pressure oxidation leaching of chalcopyrite. Part I. Comparison of high and low temperature reaction kinetics and products. *Hydrometallurgy* **2007**, *86*, 191–205. [CrossRef]
12. Flatt, J.R. The Kinetics of Pyrite and Elemental Sulfur Reactions During Nitric Acid Pre-Oxidation of Refractory Gold Ores. Ph.D. Thesis, The University of Adelaide, South Australia, Australia, 1996.
13. Gao, G.; Li, D.; Zhou, Y.; Sun, X.; Sun, W. Kinetics of high-sulphur and high-arsenic refractory gold concentrate oxidation by dilute nitric acid under mild conditions. *Miner. Eng.* **2009**, *22*, 111–115. [CrossRef]
14. Rogozhnikov, D.; Karimov, K.; Shoppert, A.; Dizer, O.; Naboichenko, S. Kinetics and mechanism of arsenopyrite leaching in nitric acid solutions in the presence of pyrite and Fe(III) ions. *Hydrometallurgy* **2021**, *199*, 105525. [CrossRef]
15. Rogozhnikov, D.A.; Mamyachenkov, S.V.; Anisimova, O.S. Nitric Acid Leaching of Copper-Zinc Sulfide Middlings. *Metallurgist* **2016**, *60*, 229–233. [CrossRef]
16. Anderson, C.G.; Harrison, K.D.; Krys, L.E. Theoretical considerations of sodium nitrite oxidation and fine grinding in refractory precious-metal concentrate pressure leaching. *Miner. Metall. Process.* **1996**, *13*, 4–11. [CrossRef]
17. Van Weert, G.; Fair, K.J.; Schneider, J.C. Prochem's NITROX Process. *CIM Bull.* **1986**, *79*, 84–85.
18. Beattie, M.J.V.; Ismay, A. Applying the redox process to arsenical concentrates. *JOM* **1990**, *42*, 31–35. [CrossRef]
19. La Brooy, S.R.; Linge, H.G.; Walker, G.S. Review of gold extraction from ores. *Miner. Eng.* **1994**, *7*, 1213–1241. [CrossRef]
20. Yildirim, Ö.; Kiss, A.A.; Hüser, N.; Leßmann, K.; Kenig, E.Y. Reactive absorption in chemical process industry: A review on current activities. *Chem. Eng. J.* **2012**, *213*, 371–391. [CrossRef]
21. Suchak, N.J.; Jethani, K.R.; Joshi, J.B. Modeling and simulation of NO_X absorption in pilot-scale packed columns. *AIChE J.* **1991**, *37*, 323–339. [CrossRef]
22. Liu, Y.; Zhang, J.; Sheng, C.; Zhang, Y.; Zhao, L. Simultaneous removal of NO and SO_2 from coal-fired flue gas by UV/H_2O_2 advanced oxidation process. *Chem. Eng. J.* **2010**, *162*, 1006–1011. [CrossRef]
23. Mamyachenkov, S.V.; Anisimova, O.S.; Kostina, D.A. Improving the precipitation of arsenic trisulfide from washing waters of sulfuric-acid production of copper smelteries. *Russ. J. Non-Ferr. Met.* **2017**, *58*, 212–217. [CrossRef]
24. Swash, P.M.; Monhemius, A.J. Synthesis, characterization and solubility testing of solids in the Ca–Fe–AsO_4 system. In Proceedings of the Sudbury '95–Mining and the Environment CANMET, Sudbury, ON, Canada, 2005; pp. 17–28.
25. Moon, D.H.; Dermatas, D.; Menounou, N. Arsenic immobilization by calcium–arsenic precipitates in lime treated soils. *Sci. Total Environ.* **2004**, *330*, 171–185. [CrossRef] [PubMed]
26. Zhu, Y.N.; Zhang, X.H.; Xie, Q.L.; Wang, D.Q.; Cheng, G.W. Solubility and Stability of Calcium Arsenates at 25 °C. *Water Air Soil Pollut.* **2006**, *169*, 221–238. [CrossRef]
27. Riveros, P.A.; Dutrizac, J.E.; Spencer, P. Arsenic Disposal Practices in the Metallurgical Industry. *Can. J. Metall. Mater. Sci.* **2001**, *40*, 395–420. [CrossRef]
28. Grebneva, A.A.; Subbotina, I.L.; Timofeev, K.L.; Maltsev, G.I. Development of Technology of Arsenic Removal from Acidic Waste Solutions in the Form of Arsenic Trisulfide. In *KnE Materials Science/IV Congress Fundamental Research and Applied Developing of Recycling and Utilization Processes of Technogenic Formations*; KnE Materials Science: Dubai, United Arab Emirates, 2020; Volume 200, pp. 209–213. [CrossRef]
29. Opio, F.K. Investigation of Fe (III)–As (III) Phases and Their Potential for Arsenic Disposal. Ph.D. Thesis, Queen's University, Kingston, ON, Canada, 2013.
30. Yao, L.; Min, X.; Xu, H.; Ke, Y.; Wang, Y.; Lin, Z.; Liang, Y.; Liu, D.; Xu, Q.; He, Y. Physicochemical and environmental properties of arsenic sulfide sludge from copper and lead−zinc smelter. *Trans. Nonferrous Met. Soc. China* **2020**, *30*, 1943–1955. [CrossRef]
31. Xu, H.; Min, X.; Wang, Y.; Ke, Y.; Yao, L.; Liu, D.; Chai, L. Stabilization of arsenic sulfide sludge by hydrothermal treatment. *Hydrometallurgy* **2020**, *191*, 105229. [CrossRef]

32. Ostermeyer, P.; Bonin, L.; Folens, K.; Verbruggen, F.; García-Timermans, C.; Verbeken, K.; Rabaey, K.; Hennebel, T. Effect of speciation and composition on the kinetics and precipitation of arsenic sulfide from industrial metallurgical wastewater. *J. Hazard. Mater.* **2021**, *409*, 124418. [CrossRef]
33. Hu, B.; Yang, T.; Liu, W.; Zhang, D.; Chen, L. Removal of arsenic from acid wastewater via sulfide precipitation and its hydrothermal mineralization stabilization. *Trans. Nonferrous Met. Soc. China* **2019**, *29*, 2411–2421. [CrossRef]
34. Rogozhnikov, D.A.; Shoppert, A.A.; Dizer, O.A.; Karimov, K.A.; Rusalev, R.E. Leaching kinetics of sulfides from refractory gold concentrates by nitric acid. *Metals* **2019**, *9*, 465. [CrossRef]
35. Rogozhnikov, D.A.; Rusalev, R.E.; Dizer, O.A.; Naboychenko, S.S. Nitric acid loosening of rebellious sulfide concentrates containing precious metals. *Tsvetnye Met.* **2018**, *12*, 38–44. [CrossRef]
36. Shahnazi, A.; Firoozi, S.; Haghshenas Fatmehsari, D. Selective leaching of arsenic from copper converter flue dust by Na_2S and its stabilization with $Fe_2(SO_4)_3$. *Trans. Nonferrous Met. Soc. China* **2020**, *30*, 1674–1686. [CrossRef]
37. Guo, F.; Wang, Q.; Demopoulos, G.P. Kinetics of iron(III)-catalyzed oxidation of arsenic(III) in acidic solutions with SO_2/O_2 gas mixture using different iron sources. *Hydrometallurgy* **2019**, *189*, 105130. [CrossRef]
38. Floroiu, R.M.; Davis, A.P.; Torrents, A. Kinetics and mechanism of As_2S_3(am) dissolution under N_2. *Environ. Sci. Technol.* **2004**, *38*, 1031–1037. [CrossRef] [PubMed]
39. Rochette, E.A.; Bostick, B.C.; Li, G.; Fendorf, S. Kinetics of Arsenate Reduction by Dissolved Sulfide. *Environ. Sci. Technol.* **2000**, *34*, 4714–4720. [CrossRef]
40. Liu, R.; Yang, Z.; He, Z.; Wu, L.; Hu, C.; Wu, W.; Qu, J. Treatment of strongly acidic wastewater with high arsenic concentrations by ferrous sulfide (FeS): Inhibitive effects of S(0)-enriched surfaces. *Chem. Eng. J.* **2016**, *304*, 986–992. [CrossRef]
41. Stephen, H.; Stephen, T. *Solubilities of Inorganic and Organic Compounds. Volume 1: Binary Systems. Part. 1*; Pergamon Press: Oxford, NY, USA, 1963; p. 975. [CrossRef]
42. Liu, J.; Wen, S.; Liu, D.; Lv, M.; Liu, L. Response surface methodology for optimization of copper leaching from a low-grade flotation middling. *Min. Metall. Explor.* **2011**, *28*, 139–145. [CrossRef]
43. Bai, X.; Wen, S.; Liu, J.; Lin, Y. Response Surface Methodology for Optimization of Copper Leaching from Refractory Flotation Tailings. *Minerals* **2018**, *8*, 165. [CrossRef]
44. Montgomery, D.C. Design and analysis of experiments. In *Environmental Progress & Sustainable Energy 32*, 8th ed.; John Wiley & Sons: Hoboken, NJ, USA, 2012. [CrossRef]
45. Zhang, G.; Chao, X.; Guo, P.; Cao, J.; Yang, C. Catalytic effect of Ag+ on arsenic bioleaching from orpiment (As_2S_3) in batch tests with Acidithiobacillus ferrooxidans and Sulfobacillus sibiricus. *J. Hazard. Mater.* **2015**, *283*, 117–122. [CrossRef] [PubMed]
46. Eary, L.E. The solubility of amorphous As_2S_3 from 25 to 90 °C. *Geochim. Cosmochim. Acta* **1992**, *56*, 2267–2280. [CrossRef]